Earth and Planetary Science Letters 421 (2015) 107–116

Contents lists available at ScienceDirect

Earth and Planetary Science Letters

www.elsevier.com/locate/epsl

Australian plate motion and topography linked to fossil New Guinea slab below Lake Eyre

W.P. Schellart [a,*], W. Spakman [b,c]

[a] School of Earth, Atmosphere and Environment, Monash University, Melbourne, VIC 3800, Australia
[b] Department of Earth Sciences, Utrecht University, Utrecht, The Netherlands
[c] Centre of Earth Evolution and Dynamics (CEED), University of Oslo, 0316 Oslo, Norway

ARTICLE INFO

Article history:
Received 5 January 2015
Received in revised form 11 March 2015
Accepted 17 March 2015
Available online 16 April 2015
Editor: J. Brodholt

Keywords:
subduction
plate tectonic reconstruction
seismic tomography
dynamic topography
New Guinea
Australia

ABSTRACT

Unravelling causes for absolute plate velocity change and continental dynamic topography change is challenging because of the interdependence of large-scale geodynamic driving processes. Here, we unravel a clear spatio-temporal relation between latest Cretaceous–Early Cenozoic subduction at the northern edge of the Australian plate, Early Cenozoic Australian plate motion changes and Cenozoic topography evolution of the Australian continent. We present evidence for a ~4000 km wide subduction zone, which culminated in ophiolite obduction and arc-continent collision in the New Guinea–Pocklington Trough region during subduction termination, coinciding with cessation of spreading in the Coral Sea, a ~5 cm/yr decrease in northward Australian plate velocity, and slab detachment. Renewed northward motion caused the Australian plate to override the sinking subduction remnant, which we detect with seismic tomography at 800–1200 km depth in the mantle under central-southeast Australia at a position predicted by our absolute plate reconstructions. With a numerical model of slab sinking and mantle flow we predict a long-wavelength subsidence (negative dynamic topography) migrating southward from ~50 Ma to present, explaining Eocene–Oligocene subsidence of the Queensland Plateau, ~330 m of late Eocene–early Oligocene subsidence in the Gulf of Carpentaria, Oligocene–Miocene subsidence of the Marion Plateau, and providing a first-order fit to the present-day, ~200 m deep, topographic depression of the Lake Eyre Basin and Murray–Darling Basin. We propound that dynamic topography evolution provides an independent means to couple geological processes to a mantle reference frame. This is complementary to, and can be integrated with, other approaches such as hotspot and slab reference frames.

1. Introduction

Large changes in absolute plate velocity of 5–15 cm/yr have been documented for several tectonic plates, such as the Indian plate and Farallon plate, and have been ascribed to changes in plate boundary forces or changes in drag forces applied by the sub-lithospheric mantle (Patriat and Achache, 1984; Schellart et al., 2010; Cande and Stegman, 2011; van Hinsbergen et al., 2011). Changes in plate boundary forces are generally linked to changes in subduction dynamics, such as initiation or termination of a subduction zone. Indeed, geodynamic subduction models show that transient subduction phases, including progressive slab lengthening (Schellart and Moresi, 2013) and slab detachment (Burkett and Billen, 2010; van Hunen and Allen, 2011), affect lithospheric plate velocities. Once detached, a slab continues to affect the Earth's surface due to its sinking into the viscous mantle, thereby producing dynamic topography (Hager et al., 1985; Gurnis et al., 1998; Braun, 2010; Heine et al., 2010; DiCaprio et al., 2011; Flament et al., 2013). Such dynamic topography is difficult to detect considering its long-wavelength, low-amplitude signal, which is superimposed on the dominant, high-amplitude, isostatically-supported topography. The Australian continent, however, forms an ideal location for investigating signals of slab-induced dynamic topography considering it is the flattest continent on Earth that sits in the middle of the Australian plate, far from current plate boundaries. Also, it has a long history of subduction along its eastern and northern margins during the Phanerozoic (Veevers, 2000; Schellart et al., 2006; Hall, 2012). These phases of subduction can impose novel constraints on absolute plate velocities if linked to mantle structure (van der Meer et al., 2010), while Australian plate motion over such slab material could induce transient dynamic topography.

* Corresponding author. Tel.: +61 3 9905 1782; fax: +61 3 9905 4903.
E-mail address: wouter.schellart@monash.edu (W.P. Schellart).

http://dx.doi.org/10.1016/j.epsl.2015.03.036

Previous work on the connection between sinking slabs and transient dynamic topography in the Australian region was either based on advection of a mantle density field derived from seismic tomography implicitly assuming (unidentified) subduction contributions (Heine et al., 2010), or on surface tectonics (Gurnis et al., 1998; DiCaprio et al., 2011). Here we provide a complete and documented account: (1) We identify latest Cretaceous–Early Cenozoic subduction north of Australia from the geological record; (2) We predict the remnant of this subduction phase to be located in the mantle under central-southeast Australia using plate tectonic reconstructions that are tied to modern absolute plate motion models; (3) We identify this slab remnant in independent seismic tomography models; and (4) We successfully predict dynamic topography change of the Australian continent during passage over the sinking slab remnant using a numerical model of slab sinking and mantle flow. Furthermore, we provide the first clear example of how long-term continental topography evolution provides new constraints on mantle reference frames of plate tectonic evolution. This new approach is complementary to, and can be integrated with, other approaches that couple geological processes and plate kinematics at the surface with the deep mantle through the use of hotspot reference frames (e.g. O'Neill et al., 2005; Doubrovine et al., 2012) or slab reference frames (e.g. van der Meer et al., 2010; Schellart, 2011; Butterworth et al., 2014).

This paper is organized as follows. After describing the numerical modelling method and the tomographic model in the Methods section, we analyze the geological evidence for latest Cretaceous to early Cenozoic subduction north of Australia. Next we cast this subduction system in several plate tectonic reconstructions of the Australia region using absolute plate positions from two modern mantle reference frames for plate tectonic evolution. Assuming vertical slab sinking, this analysis predicts slab remnants to be presently situated in the mantle under central-southeastern Australia. We identify these slab remnants in two independent tomography models of P-wave and S-wave velocity. Lastly we turn our attention to the dynamic topography evolution which Australia would have undergone as a result of passing over the sinking slab remnant where we test topography evolution as predicted form our 3-D numerical modelling with observations of present-day topography and Cenozoic topography change.

2. Methods

2.1. Numerical model

We present a numerical model that has specifically been designed to investigate the dynamic topography at the surface induced by sinking of a dense, negatively buoyant, fossil slab in the mantle. The numerical model uses the code *Underworld* (Moresi et al., 2003, 2007; Stegman et al., 2006), in which mantle flow is modelled in a three-dimensional Cartesian box by compositional buoyancy contrasts in an incompressible Boussinesq fluid at very low Reynolds number. Distinct volumes are represented by sets of Lagrangian particles that are embedded within a standard Eulerian finite element mesh, which discretizes the problem and solves the governing equations. For additional information on the numerical technique and the nondimensional equations used the reader is referred to earlier work (Moresi et al., 2003, 2007; Stegman et al., 2006). Velocities and stresses in the model are scaled following the scaling formulations presented in Schellart and Moresi (2013).

We use a Cartesian modelling domain that is 2900 km deep, which represents the entire mantle. The top surface and bottom surface have free-slip boundary conditions and represent the Earth's surface and the core–mantle boundary, respectively. Considering the low Reynolds number and the geometrical symmetry of the problem along two vertical planes (one at $x = 4000$ km and one at $z = 4000$ km), we use a box that is 4000 km long by 4000 km wide with free-slip boundary conditions at the symmetry planes, which effectively represents a modelling domain that is 8000 km long and 8000 km wide. The outer side walls (one at $x = 0$ and one at $z = 0$) have zero velocity boundary conditions. Mesh resolution in the $4000 \times 4000 \times 2900$ km^3 numerical domain is 196 (length) by 196 (width) by 160 (depth) elements, resulting in cells with spatial dimensions of 20.4 km (length) by 20.4 km (width) by 18.1 km (depth). Initial particle distribution is 20 particles per cell (total of 122,931,200 particles).

The model involves a three-dimensional layered mantle volume incorporating a dense, negatively buoyant, slab at different depth ranges from 400–800 km depth (representing the slab depth range at ~50–40 Ma) to 800–1200 km depth (present-day depth range of the slab). The anomaly is 400 km thick, 500 km wide and 1200 km long to mimic the shape of the central (high-amplitude) portion of the high-velocity anomaly we identify in our global P-wave tomography model (described in Section 5). We use a layered mantle system with a 200 km thick top layer (representing Australian continental lithosphere) with non-linear stress-dependent viscosity with maximum $\eta_{\mathrm{L(Max)}} = 500\eta_{\mathrm{UM}}$ and stress exponent $n = 3.5$ (following Mackwell et al., 1990), a 460 km thick sub-lithospheric upper mantle layer with Newtonian viscosity η_{UM} (scaling to 2.5×10^{21} Pa s in nature), and a 2240 km thick lower mantle with a three-layered Newtonian viscosity structure with $\eta_{\mathrm{LM\text{-}T}} = 10\eta_{\mathrm{UM}}$ at 660–1400 km depth, $\eta_{\mathrm{LM\text{-}M}} = 30\eta_{\mathrm{UM}}$ at 1400–2200 km depth and $\eta_{\mathrm{LM\text{-}B}} = 10\eta_{\mathrm{UM}}$ at 2200–2900 km depth. The lower mantle viscosity layering is a first-order approximation for the implied high-viscosity zone in the middle of the lower mantle (Mitrovica and Forte, 2004). We have run numerous models in which the viscosity of the plate, upper mantle and lower mantle layers have been varied, with $\eta_{\mathrm{L(Max)}} = 100$–$1000\eta_{\mathrm{UM}}$, $n = 1$–3.5, $\eta_{\mathrm{LM\text{-}T}} = 10$–$100\eta_{\mathrm{UM}}$, $\eta_{\mathrm{LM\text{-}M}} = 10$–$100\eta_{\mathrm{UM}}$, and $\eta_{\mathrm{LM\text{-}B}} = 10$–$100\eta_{\mathrm{UM}}$. The model presented in the paper (Section 6) is most in agreement with observations in terms of present day lower mantle slab sinking velocity, as well as amplitude and wavelength of surface deflection.

We use a density contrast of 33 kg/m^3 between slab and ambient mantle, which is reasonable considering a coefficient of thermal expansion of 2.4×10^{-5} K^{-1} for peridotite and a density of ~4500 kg/m^3 at 800–1200 km depth (Turcotte and Schubert, 2002), implying an average temperature contrast between ambient mantle and slab of ~306 K. We calculate the dynamic topography (surface deflection h) from the vertical normal stress at the free-slip top surface (σ_{yy}) using $\sigma_{yy} = \Delta\rho g h$, where $\Delta\rho$ is the density contrast between mantle rocks and air and g is the gravitational acceleration (Flament et al., 2013).

2.2. Seismic tomography model

We use the global P-wave mantle tomography model UU-P07 (Amaru, 2007; van der Meer et al., 2010) to investigate the mantle structure below Australia down to 2500 km depth. The global P-wave model is based on a travel time data set of ~20 million P-wave phases. The model is parameterized with constant wave-speed anomaly cells (blocks) of variable dimensions depending on the local degree by which the mantle is sampled by seismic rays (ray density) using the adaptive cell parameterization technique (Spakman and Bijwaard, 2001). The adaptive meshing technique optimizes the possibility to image detail of mantle structure exploiting the resolving power of the travel time data. Assessment of the spatial model resolution is done by sensitivity tests using synthetic velocity models of seismic wave speed (Online Supplementary Information). The resolution tests indicate that model UU-P07 can at least detect anomalies on a scale of 3° in the mantle region below Australia at a depth range of 700–1300 km.

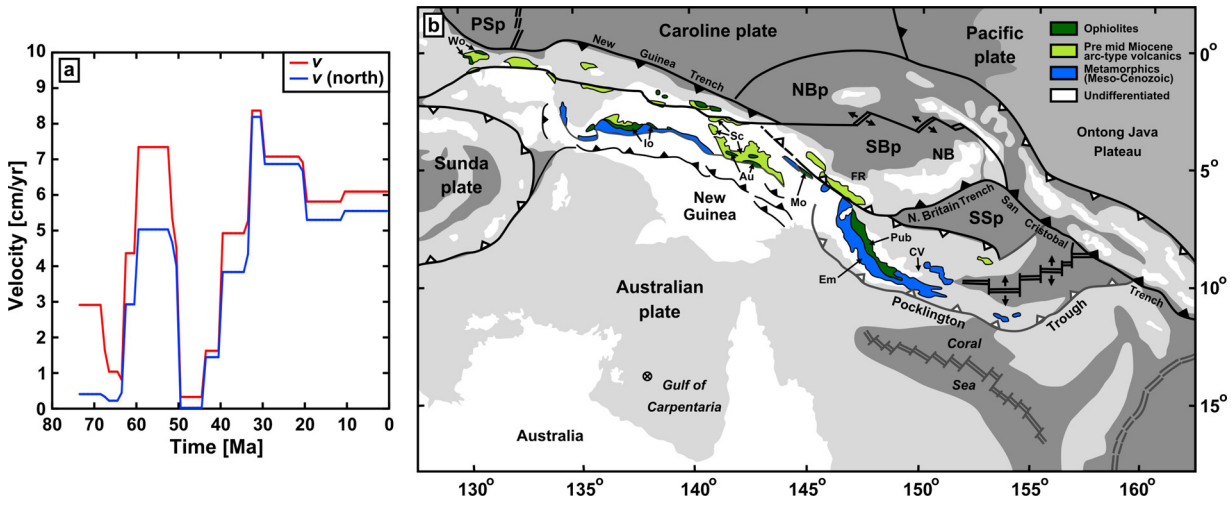

Fig. 1. Australian absolute plate velocity and New Guinea structural map. (a) Absolute velocity (red) and northward component of absolute velocity (blue) of Australian plate at 74–0 Ma for point currently located in Gulf of Carpentaria (circle with cross in (b)). Velocities were calculated in Indo–Atlantic moving hotspot reference frame (O'Neill et al., 2005) using relative plate motion model of Müller et al. (2008). (b) Geological and tectonic map of New Guinea (simplified from Davies, 2012; Baldwin et al., 2012) and surroundings. Abbreviations: Au—April ultramafics; CV—Cape Vogel; EM—Emo metamorphics; FR—Finisterre Range; Io—Irian ophiolites; Mo—Marum ophiolites; NB—New Britain; NBp—North Bismarck plate; PSp—Philippine Sea plate; Pub—Papuan ultramafic belt; SBp—South Bismarck plate; Sc—Sepik complex; SSp—Solomon Sea plate; Wo—Waigeo ophiolites. (For interpretation of the references to colour in this figure legend, the reader is referred to the web version of this article.)

3. Geological and tectonic history of New Guinea region

The Australian plate velocity record since 75 Ma shows rapid motion except for two short-lived periods at ~68–64 Ma and ~49–44 Ma (Fig. 1a). The causes for these velocity changes are unknown due to uncertainty in the geodynamic setting along the northern boundary of the Australian plate. Here we conduct a new analysis of New Guinea's geological history that proves key for answering questions on absolute plate position, velocity changes, plate motion over fossil slab remnants and the present-day long-wavelength topography of central-southeast Australia.

Metamorphic rocks, obducted ophiolites and accreted arc material are found along most of the ~2500 km long New Guinea island (Davies, 2012; Baldwin et al., 2012) (Fig. 1b) and provide constraints on the timing of collision and obduction events, and the duration and polarity of subduction preceding obduction. Structural investigations of the largest ophiolite unit in New Guinea (the Papuan Ultramafic belt) imply southwest-directed obduction on top of the Emo metamorphics, whose geochemistry points to a backarc origin (Worthing and Crawford, 1996), during the terminal stage of a northeast-dipping subduction zone (Davies and Warren, 1992; Davies, 2012). Additional evidence for this fossil subduction zone is represented by the Pocklington Trough (Fig. 1b), a ~1600 km bathymetric feature interpreted as a fossil north to northeast-dipping subduction zone (Schellart et al., 2006; Davies, 2012; Baldwin et al., 2012). The supra-subduction zone (forearc) origin of (part of) the ophiolites and their Maastrichtian age (based on microfossils; Belford, 1976) imply northeast-directed subduction initiation at ~71–65 Ma. Furthermore, Paleocene metamorphics of the subduction complex (Davies and Warren, 1992) and ~59 Ma arc volcanics at Cape Vogel (Walker and McDougall, 1982) imply north to northeast-dipping Paleocene subduction.

The ~58 Ma metamorphic sole of the ophiolite (Lus et al., 2004) indicates that obduction and subduction termination in this belt occurred after ~58 Ma. Subduction termination is further constrained by termination of spreading in the Coral Sea located south of the Pocklington Trough (Fig. 1b), which is dated at ~52 Ma (Gaina et al., 1999). Considering the close spatial proximity (200–400 km) of the central Pocklington Trough and the fossil Coral Sea spreading centre and their comparable strike (~WNW–ESE), termination of spreading can be ascribed to contemporaneous subduction termination and collision, and subsequent slab detachment at the Pocklington Trough.

Ophiolites and underlying metamorphics in western-central New Guinea imply the former existence of a north-dipping subduction zone that terminated in the latest Cretaceous or Early Cenozoic (Davies and Warren, 1992; Baldwin et al., 2012) (Fig. 1b). The geological evidence has led Hall (2012) to propose a north-dipping ~65–50 Ma subduction zone north of western-central New Guinea with subduction termination at ~50 Ma during collision of the Sepik arc.

The accumulated geological evidence, together with the temporal overlap of subduction in western-central New Guinea (~65–50 Ma) and the eastern New Guinea–Pocklington region (~71–52 Ma), their close spatial proximity (the nearest ophiolite fragments of both subduction segments are currently separated by only ~120 km, Fig. 1b), and their identical polarity, imply the existence of one continuous ~4000 km wide, north-dipping subduction zone. We will call this zone the New Guinea–Pocklington subduction zone, which was active at ~71–65 Ma to 52–50 Ma and culminated in collision of the Sepik-Cape Vogel arc with the New Guinea passive margin and south to southwest-directed obduction of ophiolites. Using these geological constraints and constraints from absolute plate motion models, we present a reconstruction of the New Guinea–Pocklington subduction zone, illustrating its geographical position from 70 Ma to present with respect to the Indo–Atlantic moving hotspot reference frame (O'Neill et al., 2005; Müller et al., 2008) (Fig. 2), which we have used successfully before to explain deep mantle structure (Schellart, 2011; Schellart and Spakman, 2012). We also present our reconstruction in a recent global moving hotspot reference frame (Doubrovine et al., 2012) (Fig. 3).

4. Plate tectonic reconstruction of New Guinea region

The north-dipping New Guinea–Pocklington subduction zone formed at ~71–65 Ma in a backarc basin (Emo backarc Basin), as implied by the geochemistry of the Emo metamorphic rocks found below the Papuan ophiolite (Worthing and Crawford, 1996) (Fig. 2a–b). These Emo metamorphics originate from backarc oceanic lithosphere that has been subducted along the Pocklington subduction segment. During subduction initiation, northward Australian plate motion was very slow (~0.2–0.4 cm/yr, Fig. 1a).

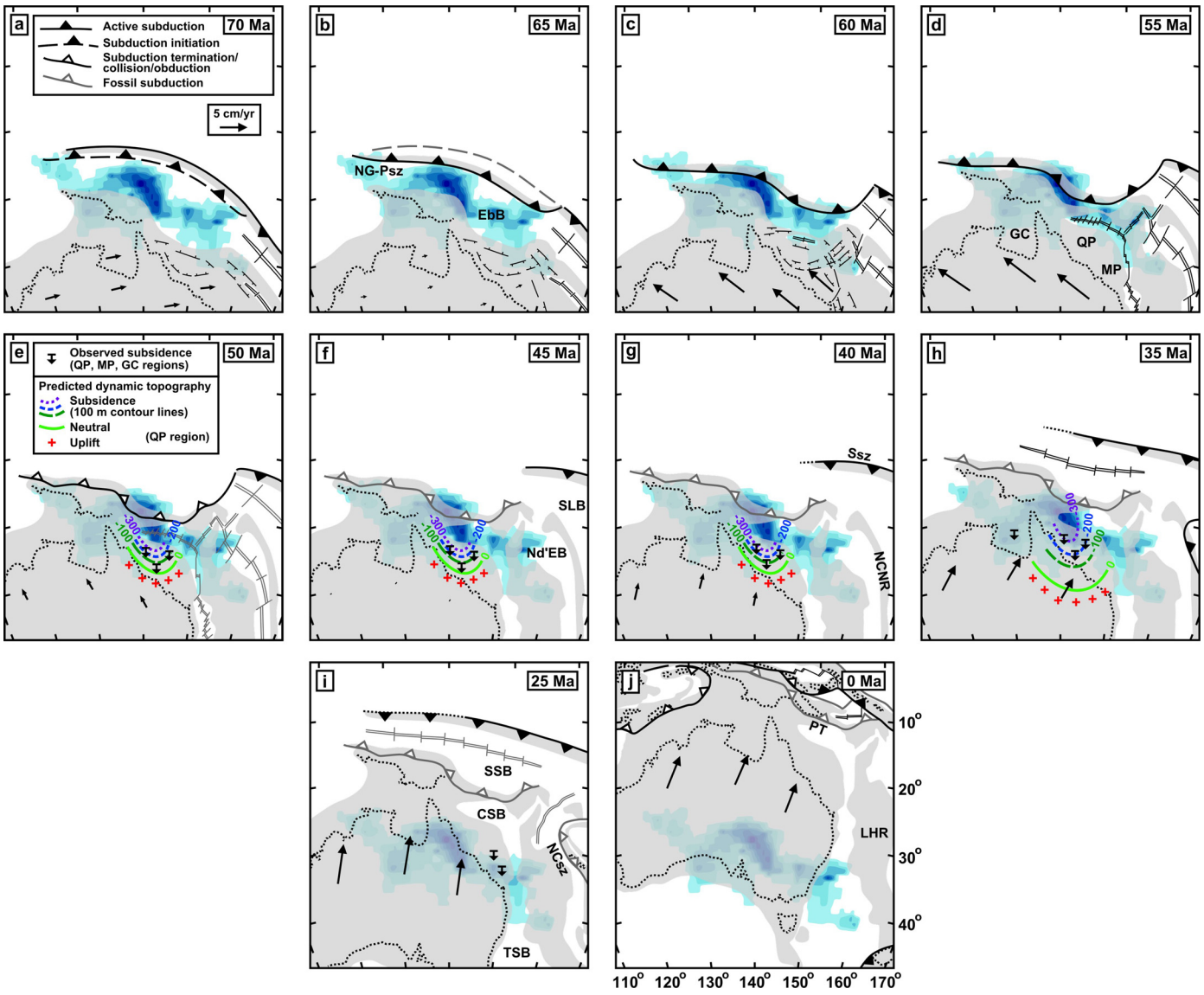

Fig. 2. Plate tectonic reconstructions of the Australia–New Guinea region at 70–0 Ma, illustrating the evolution of the north-dipping New Guinea–Pocklington subduction zone in an Indo–Atlantic hotspot reference frame. Blue area outlines the isolated high-velocity P-wave anomaly at 900 km depth below Australia (see Fig. 4c), interpreted as the fossil New Guinea–Pocklington slab. An absolute plate motion model (O'Neill et al., 2005; Müller et al., 2008) was used to constrain Australian plate motion in an Indo–Atlantic moving hotspot reference frame. For the reconstruction in a global moving hotspot reference frame (Doubrovine et al., 2012) see Fig. 3. Velocity vectors are averaged for 2 Myr periods except for (j), which is averaged for 1 Myr. Evolution of the region located east of Australia is based on Gaina et al. (1999), Schellart et al. (2006) and Schellart and Spakman (2012). Observed subsidence for Queensland Plateau, Marion Plateau and Gulf of Carpentaria is indicated. Dynamic topography in the Queensland Plateau region as predicted by a numerical model of slab sinking and mantle flow (see Fig. 7) is indicated with the dark green, blue and purple lines (subsidence) and red crosses (uplift). Note that in these reconstructions the predicted dynamic topography in the Queensland plateau (subsidence) matches observations (subsidence) at 50–35 Ma very well. Abbreviations: CSB—Coral Sea Basin; EbB—Emo backarc Basin; GC—Gulf of Carpentaria; LHR—Lord Howe Rise; MP—Marion Plateau; NCNR—New Caledonia–Norfolk Ridge; NCsz—New Caledonia subduction zone; Nd'EB—North d'Entrecasteaux Basin; NG–Psz—New Guinea–Pocklington subduction zone; PT—Pocklington Trough; QP—Queensland Plateau; SLB—South Loyalty Basin; SSB—Solomon Sea Basin; Ssz—Solomon subduction zone; TSB—Tasman Sea Basin. (For interpretation of the references to colour in this figure legend, the reader is referred to the web version of this article.)

From ~64–59 Ma Australian plate velocity increased rapidly with its northward component increasing to ~5 cm/yr. Such an increase is consistent with an increase in slab pull from the New Guinean–Pocklington slab due to progressive slab lengthening. Indeed, generic subduction models (Schellart and Moresi, 2013; Schellart et al., 2010) demonstrate that during the initial transient subduction stage, the subducting plate velocity can increase by ~6 cm/yr within 10 Myr, comparable to the velocity jump for the Australian plate. The west-directed velocity component of the Australian plate is consistent with additional slab pull along the west-northwest-dipping West Sulawesi subduction zone in the northwestern corner of the Australian plate that was active at 65–50 Ma (Hall, 2012). Considering that at 71–52 Ma the Australian plate had spreading ridges along its western, southern and eastern boundaries (Royer and Sandwell, 1989; Gaina et al., 1999; Müller et al., 2008), we can confidently link the plate acceleration at 64–59 Ma, and the rapid plate motion at 59–52 Ma to the slab pull from the New Guinea–Pocklington and the West Sulawesi subduction zones in the north. Rapid Australian plate motion continued until ~52 Ma, when northward velocities decreased to ~0 cm/yr at ~49 Ma (Fig. 1a). The slowdown coincides with our proposed time of subduction termination and arc-continent collision at 52–50 Ma followed by loss of slab pull due to wholesale slab detachment.

At 44–40 Ma, Australia rapidly accelerated ~north-northeastward, closely coinciding with subduction initiation and progressive

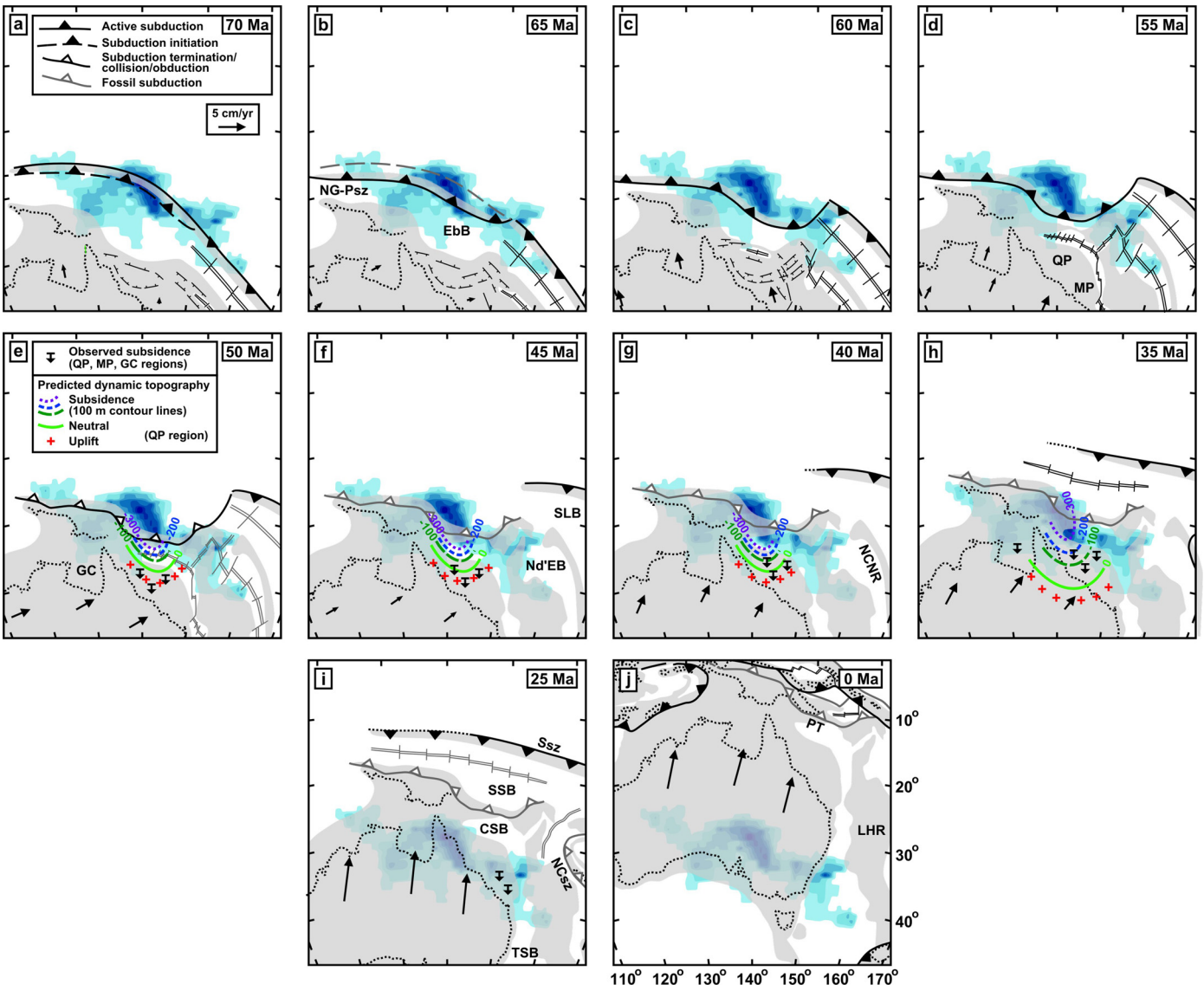

Fig. 3. Plate tectonic reconstructions of the Australia–New Guinea region at 70–0 Ma, illustrating the evolution of the north-dipping New Guinea–Pocklington subduction zone in a global hotspot reference frame. The relative plate motion model from Müller et al. (2008) and the global moving hotspot reference frame from Doubrovine et al. (2012) were used to constrain the absolute motion of the Australian plate (cf. Fig. 2 using the Indo–Atlantic moving hotspot reference frame from O'Neill et al., 2005). Blue area outlines the isolated high-velocity P-wave anomaly at 900 km depth below Australia (see Fig. 4c), interpreted as the fossil New Guinea–Pocklington slab. Velocity vectors are averaged for 2 Myr periods except for (j), which is averaged for 1 Myr. Evolution of the region located east of Australia is based on Gaina et al. (1999), Schellart et al. (2006) and Schellart and Spakman (2012). Observed subsidence for Queensland Plateau, Marion Plateau and Gulf of Carpentaria is indicated. Dynamic topography in the Queensland Plateau region as predicted by a numerical model of slab sinking and mantle flow (see Fig. 7) is indicated with the dark green, blue and purple lines (subsidence) and red crosses (uplift). Note that in these reconstructions the predicted dynamic topography in the Queensland plateau (uplift) does not match observations (subsidence) at 50–40 Ma. Only at 35 Ma is there agreement. Abbreviations: CSB—Coral Sea Basin; EbB—Emo backarc Basin; GC—Gulf of Carpentaria; LHR—Lord Howe Rise; MP—Marion Plateau; NCNR—New Caledonia-Norfolk Ridge; NCsz—New Caledonia subduction zone; Nd'EB—North d'Entrecasteaux Basin; NG–Psz—New Guinea–Pocklington subduction zone; PT—Pocklington Trough; QP—Queensland Plateau; SLB—South Loyalty Basin; SSB—Solomon Sea Basin; Ssz—Solomon subduction zone; TSB—Tasman Sea Basin. (For interpretation of the references to colour in this figure legend, the reader is referred to the web version of this article.)

slab lengthening at the North Sulawesi–Halmahera and Sunda subduction zones in the north (Hall, 2012) and the New Caledonia subduction zone in the northeast (Schellart et al., 2006) (Figs. 1a, 2f–i). This caused Australia to override the fossil New Guinea–Pocklington slab (Fig. 2g–j), which sank deeper into the mantle.

5. Deep mantle structure below Australia

The key prediction we make from the absolute plate reconstructions is that the detached slab should currently be found under central-southeast Australia (Fig. 2). Furthermore, we predict a ~500–1400 km depth location for the fossil slab by combining a ~71–50 Ma subduction period and recent estimates of average slab sinking rates in the mantle (~1–2 cm/yr) (van der Meer et al., 2010; Schellart and Spakman, 2012; Butterworth et al., 2014). Using the global P-wave mantle tomography model UU-P07 (Amaru, 2007), we identify an isolated positive velocity anomaly at ~800–1200 km depth under central-southeast Australia of comparable lateral extent (~4000 km) and similar orientation (~WNW–ESE) as the New Guinea–Pocklington subduction zone (Figs. 2, 4b–f). Notably, the shape of the central (NW–SE striking) and eastern (E–W striking) parts of the anomaly at 900 km depth (Fig. 4c) mimic the shape of the Pocklington Trough (Fig. 1b).

The existence of the anomaly is corroborated by resolution analyses and by detection in independent tomography model S40RTS (Ritsema et al., 2011). A comparison between the global P-wave tomography model UU-P07 used here and the global S-wave

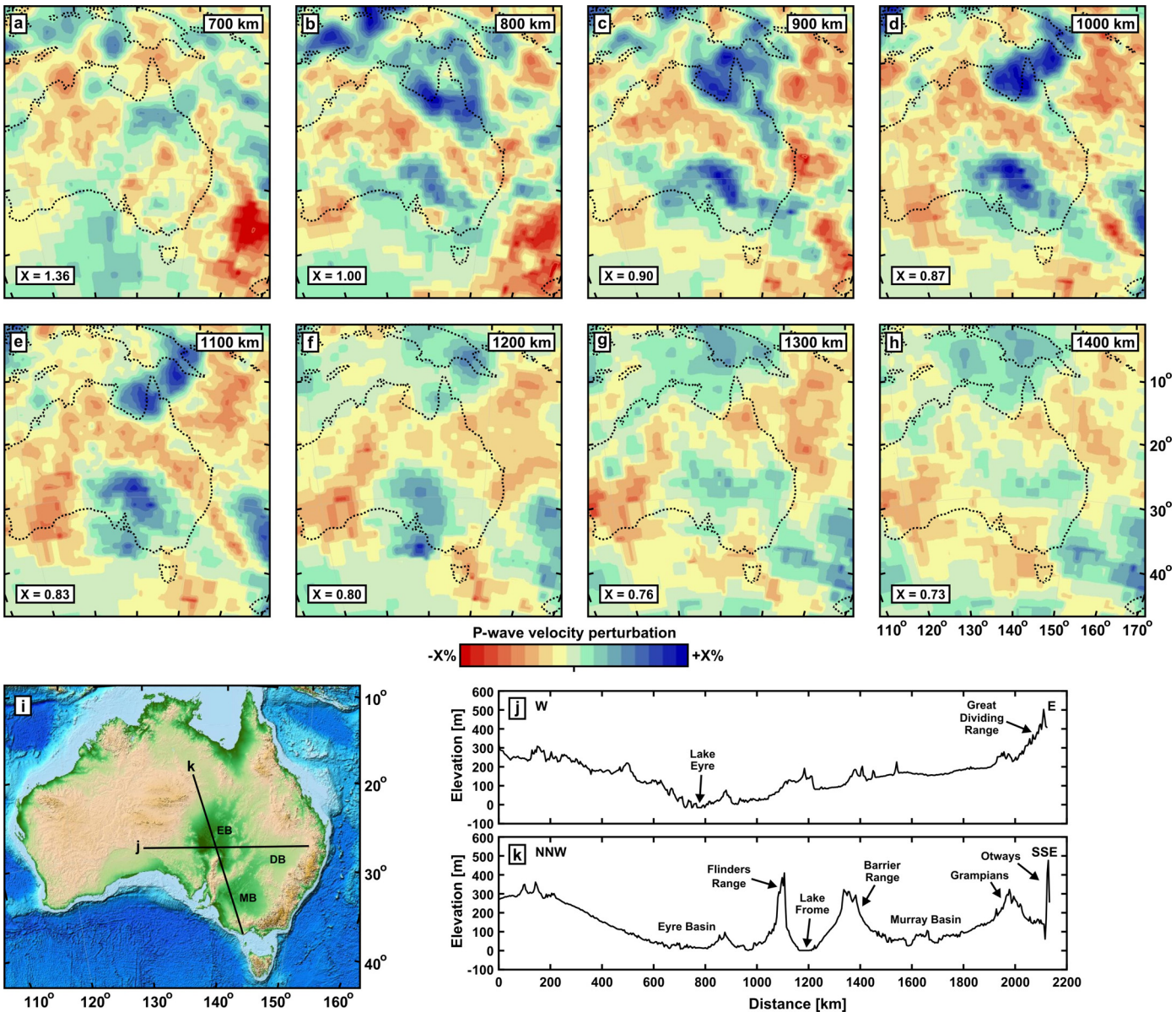

Fig. 4. Mantle tomography and topography in the Australia–New Guinea region. (a)–(h) Horizontal slices of global P-wave tomography model UU-P07 (Amaru, 2007; van der Meer et al., 2010) at 700–1400 km depth. Note location of the high-velocity anomaly (interpreted as the fossil New Guinea–Pocklington slab) in (b)–(f) below central-southeast Australia, which is also detected in S-wave tomography model S40RTS (Ritsema et al., 2011) (Fig. 5). The high-velocity anomaly below northernmost Australia, the Gulf of Carpentaria and eastern New Guinea is discussed elsewhere (Hall and Spakman, 2002; Schellart and Spakman, 2012). (i) Topography of Australia (ETOPO1 model). (j) East–west section showing topographic elevation across Eyre Basin. (k) Northwest–southeast section showing topographic elevation across Eyre Basin – Murray–Darling Basin. Locations of cross-sections are shown in (i). Abbreviations: DB—Darling Basin; EB—Eyre Basin; MB—Murray Basin.

tomography model S40RTS is presented in Fig. 5 for two mantle depths (1000 and 1200 km). Data, model parameterization and inversion technique applied and target seismic wave velocity fields are all independent between these two models. As a result, the strong correspondence between the two independent models serves as an existence proof for mantle structure that is imaged. As can readily be observed the larger scale patterns correspond rather well, including the positive anomaly under central-southeast Australia. We add that the anomaly is also observed in other global mantle seismic tomography models, for example the recent P-wave model from Simmons et al. (2012).

Our identification of the fossil slab anomaly holds if slab sinking was predominantly vertical (van der Meer et al., 2010; Schellart and Spakman, 2012). Such sub-vertical sinking is likely, considering that trench migration is minor in both reconstructions (Figs. 2 and 3). Indeed, geodynamic subduction models indicate that slab sinking occurs sub-vertically when trench migration is small (Kincaid and Olson, 1987; Schellart, 2011), forming a folded slab pile that sinks into the lower mantle. Such folded slab piles are more likely to retain their trench-parallel orientation than in the case where the slab would flatten in the mantle transition zone.

The central portion of the anomaly is most pronounced with a depth extent of 800–1200 km. This portion corresponds to the western Pocklington Trough subduction segment that has accommodated the largest amount of subduction (~1100 km, Fig. 2); it strikes NW–SE, is ~1200 km long and is located below the Eyre and Murray–Darling basins. The western and eastern parts of the anomaly are less pronounced and have a smaller depth range (~800–1000 km), and correspond to subduction segments that have accommodated smaller amounts of subduction, in particular the western part with ~600–700 km of subduction.

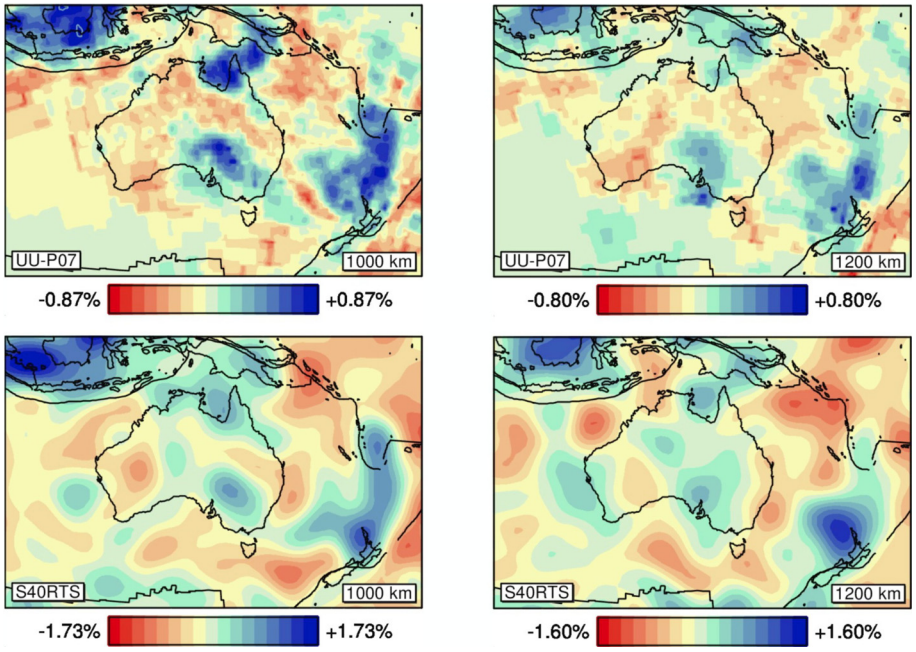

Fig. 5. Comparison between model UU-P07 (Amaru, 2007) (used here) and S40RTS (Ritsema et al., 2011) for two mantle depths, 1000 and 1200 km. Data, model parameterization and inversion technique applied and target seismic wave velocity fields (P-velocity and S-velocity, respectively) are all independent between these two models. As a result strong correspondence between the two independent models serves as an existence proof for mantle structure that is imaged. As can readily be observed the larger scale patterns correspond rather well. The positive anomaly under central-southeast Australia, subject of our research, is imaged in both models. Note that the details of spatial resolution (linear dependence between model parameters; lateral and vertical smearing effects) in both models can be quite different. UU-P07 can at least detect anomalies on a scale of 3° in this mantle region (see supplementary material), while the lateral resolution in model S40RTS is optimally ∼4.5°.

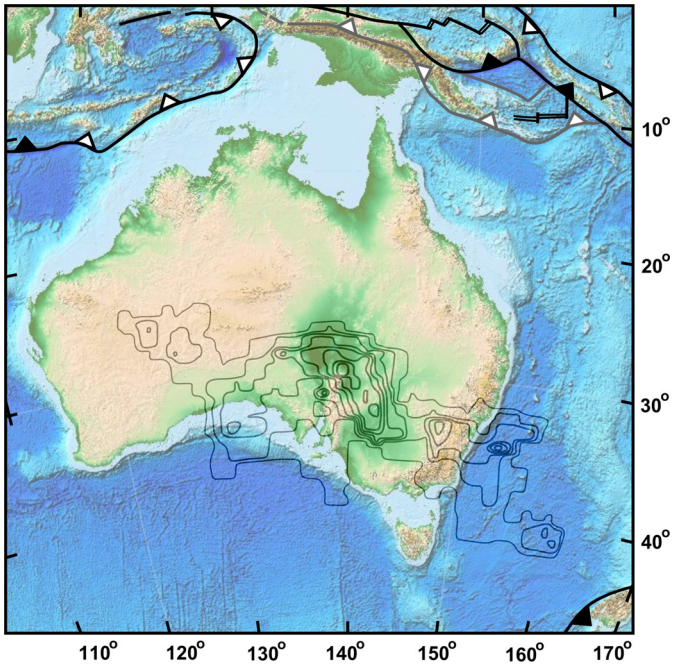

Fig. 6. Topography of Australia (ETOPO1 model) and outlines of the isolated P-wave high-velocity anomaly below central and southeastern Australia (at 900 km depth shown in Fig. 4c). Note that the central, high-amplitude, part of the anomaly (at 135–144°E and 26–35°S) is located directly below the lowest parts of the Eyre and Murray basins (in green). (For interpretation of the references to colour in this figure legend, the reader is referred to the web version of this article.)

6. Dynamic topography evolution of the Australian region

It is conspicuous that the high-velocity anomaly, in particular its high-amplitude (western Pocklington) portion, sits vertically below the Eyre–Murray–Darling depression (Fig. 6). This depression consists of the Lake Eyre Basin, one of the largest internally drained basins in the world (Habeck-Fardy and Nanson, 2014) and the Murray–Darling Basin, named after the largest river system in Australia. The close spatial overlap between the high-velocity anomaly and the depression suggests that downward-directed mantle flow induced by slab sinking generates subsidence above the slab, as has been proposed previously for other regions overlying sinking fossil slabs (Hager et al., 1985; Gurnis et al., 1998; Braun, 2010; Heine et al., 2010; DiCaprio et al., 2011; Flament et al., 2013). East–west and northwest–southeast profiles illustrate that the Eyre–Murray–Darling depression has a characteristic long-wavelength length scale of ∼2000–2500 km (Fig. 4i–k). Short length scale (∼100–300 km), high-amplitude, perturbations such as the Flinders Range superimposed on the long wavelength depression (Fig. 4k) can be attributed to active east–west intraplate compression and local crustal shortening (Sandiford and Quigley, 2009).

We have constructed a geodynamic model of mantle flow using the numerical code *Underworld* (Moresi et al., 2003, 2007) to investigate the amplitude and length scale of dynamic topography due to fossil slab sinking. For the present day, with a lower mantle slab at 800–1200 km depth, we obtain a slab sinking velocity of 0.85 cm/yr, in agreement with predictions from the reconstruction (0.6–1.0 cm/yr), and a dynamic topography amplitude of −200 m (subsidence) centrally above the slab (Fig. 7). The negative dynamic topography has a typical length scale of ∼2500 km by ∼3000 km (Fig. 7b), comparable with the Eyre–Murray–Darling depression (Fig. 4i–k).

Considering that the Australian plate has moved rapidly north–northeastward since ∼40 Ma, we predict that the subsidence has migrated south–southwestward over the Australian plate. For the period 50–30 Ma, our reconstructions predicts a slab location below the Coral Sea and Gulf of Carpentaria regions (Fig. 2e–h) at ∼400–800 to 500–900 km depth while our numerical model predicts a maximum subsidence of ∼360–500 m (Fig. 7b). This can explain Eocene–Oligocene subsidence of the Queensland Plateau

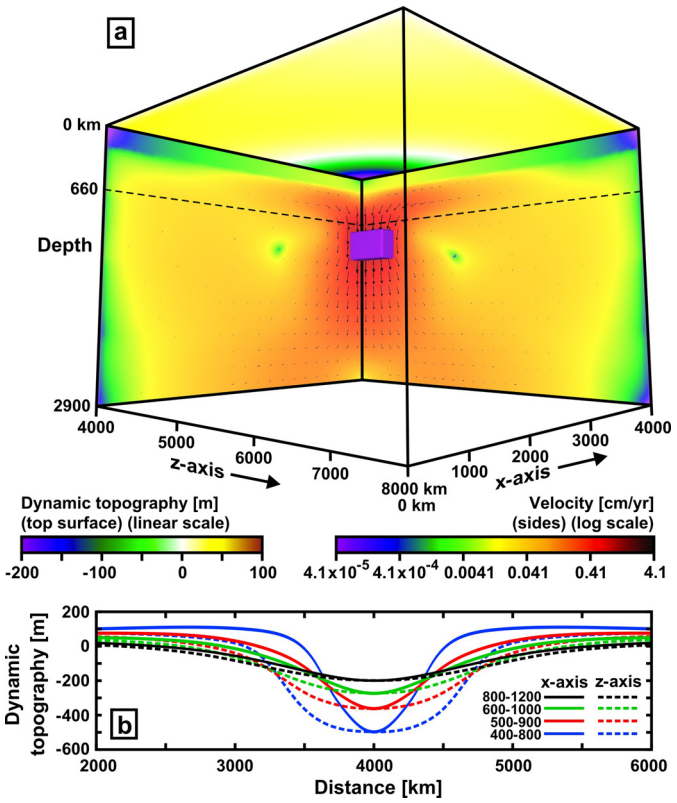

Fig. 7. Geodynamic model of mantle flow and dynamic topography at the surface induced by sinking of a slab volume located in the mantle using *Underworld*. The slab volume is 1200 km long, 500 km wide and 400 km thick and represents a first order approximation of the fossil slab segment below the Eyre and Murray–Darling basins in central-southeast Australia. Density contrast between slab and ambient mantle in the model is 33 kg/m^3 and upper mantle viscosity $\eta_{UM} = 2.5 \times 10^{21}$ Pa s. (a) 3D view with sinking slab (in purple) at 800–1200 km depth, velocity field (vertical symmetry planes) and dynamic topography (top surface). (b) Dynamic topography at the top surface along two profiles with one along the x-axis (continuous lines, $z = 4000$ km) and one along the z-axis (dashed lines, $x = 4000$ km), and for four different slab depths: 800–1200 km (black, present), 600–1000 km (green, ~25 Ma), 500–900 km (red, 35–30 Ma), 400–800 km (blue, 50–40 Ma). (For interpretation of the references to colour in this figure legend, the reader is referred to the web version of this article.)

(Isem et al., 1984–1996), as well as the phase of rapid subsidence (~330 m) at ~37–30 Ma documented in the Gulf of Carpentaria (Heine et al., 2010) (Fig. 2e–h). Our reconstruction at ~25 Ma predicts that the slab is located below the Great Dividing Range in Queensland and below the Marion Plateau (Fig. 2i) at ~600–1000 km depth, implying maximum subsidence of ~270 m (Fig. 6b). Significant subsidence is indeed recorded in the Marion Plateau since 30 Ma (Isem et al., 1984–1996), while continental sedimentation in the Queensland region of the Great Dividing Range could imply subsidence there. Although one would expect moderate uplift of the northern regions after passing over the slab anomaly, this is not observed. This can be explained by the increasing influence of subducted slab material of the Melanesian and Sunda subduction zones in the north (Sandiford, 2007), as predicted by geodynamic models (DiCaprio et al., 2011), inducing regional dynamic topography of ~100–300 m at 32–10 Ma.

The region of the current Lake Eyre Basin has experienced erosion and weathering in the Late Cretaceous–earliest Eocene (~99–55 Ma) and late Eocene–late Oligocene (~41–24) Ma (Alley, 1998), implying that the basin as we know it today would only have started to form in or after the latest Oligocene/Miocene (after ~25 Ma). This is consistent with our model predictions, illustrating that at 25 Ma the southern part of the anomaly was located below the northernmost part of the Eyre Basin (Fig. 2i). Earlier phases of sedimentation in the region that is now occupied by the Eyre Basin, namely before ~99 Ma and between ~55 Ma and ~41 Ma, might be associated with other processes (e.g. eustatic processes) or with dynamic topography induced by older slabs. We emphasize that these earlier sedimentation phases do not imply that the Eyre Basin, with its characteristic internal drainage, already existed at these earlier times.

Subsidence data for the Murray Basin region (Heine et al., 2010) show minor subsidence from 30 to 10 Ma (~40 m) followed by more significant subsidence from 10 Ma to ~1.5 Ma (120 m). This can be explained by the Murray region moving towards and over the anomaly in the last 30 Myr. Finally, geological evidence indicates south to southwestward migration of Lake Eyre during the Quaternary (DeVogel et al., 2004; Sandiford and Quigley, 2009), in agreement with our predictions.

7. Dynamic topography provides new constraints on mantle reference frames

The confined north–south extent of the slab anomaly suggests minor trench migration, which complies with general kinematic aspects of subduction zones with a relatively large (trench-parallel) width (3000–5000 km), as predicted by geodynamic subduction models (Schellart et al., 2010). These models demonstrate that subducting plate motion is relatively fast (5–6 cm/yr), as observed (Fig. 1a), and that subduction occurs mostly (65–80%) through trenchward subducting plate motion, with a smaller subduction component (20–35%) through trench retreat. Our reconstructions in the Indo–Atlantic hotspot reference frame (Fig. 2) and global hotspot reference frame (Fig. 3) allow ~10–30% and ~25–40% of subduction through trench rollback, respectively, both in accordance with predictions.

Moderate spatial shifts observed between the two reference frames (cf. Figs. 2 and 3), combined with uncertainty in subduction zone geometry at 71–50 Ma, do not allow us to distinguish between the two frames. Combining the reconstructions with tomography and predicted dynamic topography, however, does, as we can predict the timing of onset of slab-sinking-induced surface subsidence in the two reference frames. Notably, the two frames have a ~250–400 km latitudinal shift in the Coral Sea region at 50–35 Ma (cf. Fig. 2e–h and Fig. 3e–h). Slab-sinking-induced subsidence of the Queensland plateau is predicted to start at ~50 Ma in the Indo–Atlantic hotspot reference frame (Fig. 2e), in agreement with observations of major subsidence since ~52 Ma (Isem et al., 1984–1996). In the global hotspot reference frame, the Queensland Plateau is located too far south (~400 km) with respect to the slab anomaly at 50 Ma to cause subsidence of the Queensland Plateau and instead uplift is predicted, in disagreement with observations (Fig. 3e). At 45 Ma and 40 Ma, the Queensland Plateau is still located too far south (~200–300 km, Fig. 3f, g) and the global frame predicts subsidence of the entire Queensland Plateau to start only at ~35 Ma (Fig. 3h).

With the above example we illustrate for the first time how dynamic topography evolution, when combined with plate tectonic reconstructions, mantle tomography and geodynamic models, provides an independent constraint on the mantle reference frame of plate tectonic evolution. Although it is conceivable that a future "dynamic topography mantle reference frame" may become reality, it is also a valuable approach to use accurate topography evolution as new information to constrain and refine existing mantle reference frames based on hotspots (e.g. O'Neill et al., 2005; Doubrovine et al., 2012) and slabs (e.g. van der Meer et al., 2010; Schellart, 2011; Butterworth et al., 2014).

8. Conclusions

Our geological compilation of the New Guinea region, our plate tectonic reconstructions (Figs. 2 and 3) and our discovery of the high-velocity lower mantle anomaly below central-southeastern Australia (Figs. 4 and 5) provide strong support for the existence of a large ~4000 km wide, ~north-dipping subduction zone that was active at ~71–50 Ma along the northern margin of the Australian plate. We argue that this subduction zone was responsible for the speed-up of the Australian plate at ~64–59 Ma during slab lengthening, for fast velocities at ~59–52 Ma, and for the slowdown at ~52–49 Ma during subduction termination (Fig. 1a). We further propose that subduction termination induced south to southeast-directed ophiolite obduction on top of the New Guinea continental crust, caused arc-continent collision, triggered termination of spreading in the Coral Sea and led to detachment of the subducted slab. We argue that further sinking of the detached slab caused south to southwestward migration of long-wavelength, low-amplitude, subsidence induced by the sinking slab remnant as Australia moved north to northeastward over the fossil slab, explaining subsidence of the Queensland Plateau, Gulf of Carpentaria and Marion Plateau. Currently, the slab is found in the lower mantle below the Eyre–Murray–Darling depression and we propose that this depression is the direct result of the sinking slab as implied by the close spatial overlap between the depression and the high-velocity anomaly (Fig. 6) and by our geodynamic model of slab sinking and mantle flow, which predicts a long-wavelength, low-amplitude, depression (Fig. 7b), comparable with observations (Fig. 4i–k). Our geodynamic model also predicts a lower mantle slab sinking velocity of 0.85 cm/yr, which is in agreement with predictions from our reconstructions (~0.6–1.0 cm/yr).

Finally, by presenting our reconstructions in two absolute reference frames, an Indo–Atlantic moving hotspot reference frame (Fig. 2) and a global moving hotspot reference frame (Fig. 3), we demonstrate that dynamic topography evolution provides an independent means to couple geological processes to a mantle reference frame. This new approach is complementary to, and can be integrated with, other approaches such as hotspot and slab reference frames.

Acknowledgements

We thank Jeroen Ritsema and an anonymous reviewer for helpful and constructive comments. W.P.S. was supported with a Future Fellowship (FT110100560) from the Australian Research Council and with computational resources from the NCI National Facility through the National Computational Merit Allocation Scheme (project ei8). W.S. was partly supported by the Research Council of Norway through its Centres of Excellence funding scheme, project number 223272.

Appendix A. Supplementary material

Supplementary material related to this article can be found online at http://dx.doi.org/10.1016/j.epsl.2015.03.036.

References

Alley, N.F., 1998. Cainozoic stratigraphy, palaeoenvironments and geological evolution of the Lake Eyre Basin. Palaeogeogr. Palaeoclimatol. Palaeoecol. 144, 239–263.

Amaru, M., 2007. Global travel time tomography with 3-D reference models. PhD. Utrecht University. Available at: http://igitur-archive.library.uu.nl/dissertations/2007-0202-201924/index.html.

Baldwin, S.L., Fitzgerald, P.G., Webb, L.E., 2012. Tectonics of the New Guinea region. Annu. Rev. Earth Planet. Sci. 40, 495–520.

Belford, D., 1976. Foraminifera and age of samples from Southeastern Papua. Bull. - Aust., Bur. Miner. Resour., Geol. Geophys. 165.

Braun, J., 2010. The many surface expressions of mantle dynamics. Nat. Geosci. 3, 825–833. http://dx.doi.org/10.1038/ngeo1020.

Burkett, E.R., Billen, M.I., 2010. Three dimensionality of slab detachment due to ridge trench collision: laterally simultaneous boudinage versus tear propagation. Geochem. Geophys. Geosyst. 11, Q11012. http://dx.doi.org/10.1029/2010GC003286.

Butterworth, N.P., Talsma, A.S., Müller, R.D., Seton, M., Bunge, H.-P., Schuberth, B.S.A., Shephard, G.E., Heine, C., 2014. Geological, tomographic, kinematic and geodynamic constraints on the dynamics of sinking slabs. J. Geodyn. 73, 1–13. http://dx.doi.org/10.1016/j.jog.2013.10.006.

Cande, S.C., Stegman, D.R., 2011. Indian and African plate motions driven by the push force of the Reunion plume head. Nature 475, 47–52. http://dx.doi.org/10.1038/nature10174.

Davies, H.L., 2012. The geology of New Guinea – the cordilleran margin of the Australian continent. Episodes 35, 87–102.

Davies, H.L., Warren, R.G., 1992. Eclogites of the D'Entrecaseaux Islands. Contrib. Mineral. Petrol. 112, 463–474.

DeVogel, S.B., Magee, J.W., Manley, W.F., Miller, G.H., 2004. A GIS-based reconstruction of late Quaternary paleohydrology: Lake Eyre, arid central Australia. Palaeogeogr. Palaeoclimatol. Palaeoecol. 204, 1–13. http://dx.doi.org/10.1016/S0031-0182(03)00690-4.

DiCaprio, L., Gurnis, M., Müller, R.D., Tan, E., 2011. Mantle dynamics of continentwide Cenozoic subsidence and tilting of Australia. Lithosphere 3, 311–316. http://dx.doi.org/10.1130/L140.1.

Doubrovine, P.V., Steinberger, B., Torsvik, T.H., 2012. Absolute plate motions in a reference frame defined by moving hot spots in the Pacific, Atlantic, and Indian oceans. J. Geophys. Res. 117, B09101. http://dx.doi.org/10.1029/2011JB009072.

Flament, N., Gurnis, M., Müller, R.D., 2013. A review of observations and models of dynamic topography. Lithosphere 5, 189–210. http://dx.doi.org/10.1130/L245.1.

Gaina, C., Müller, R.D., Royer, J.-Y., Symonds, P., 1999. Evolution of the Louisiade triple junction. J. Geophys. Res. 104, 12927–12940.

Gurnis, M., Müller, R.D., Moresi, L., 1998. Cretaceous vertical motion of Australia and the Australian–Antarctic discordance. Science 279, 1499–1504.

Habeck-Fardy, A., Nanson, G.C., 2014. Environmental character and history of the Lake Eyre Basin, one seventh of the Australian continent. Earth-Sci. Rev. 132, 39–66. http://dx.doi.org/10.1016/j.earscirev.2014.02.003.

Hager, B.H., Clayton, R.W., Richards, M.A., Comer, R.P., Dziewonski, A.M., 1985. Lower mantle heterogeneity, dynamic topography and the geoid. Nature 313, 541–545.

Hall, R., 2012. Late Jurassic–Cenozoic reconstructions of the Indonesian region and the Indian Ocean. Tectonophysics 570–571, 1–41. http://dx.doi.org/10.1016/j.tecto.2012.04.021.

Hall, R., Spakman, W., 2002. Subducted slabs beneath the eastern Indonesia–Tonga region; insights from tomography. Earth Planet. Sci. Lett. 201, 321–336.

Heine, C., Müller, R.D., Steinberger, B., DiCaprio, L., 2010. Integrating deep Earth dynamics in paleogeographic reconstructions of Australia. Tectonophysics 483, 135–150. http://dx.doi.org/10.1016/j.tecto.2009.08.028.

Isem, A.R., Langford, R.P., Truswell, E.M., Wilford, G.E., 1984–1996. Cainozoic Era, Paleogeographic Atlas of Australia, vol. 10. Australian Geological Survey Organization, Canberra.

Kincaid, C., Olson, P., 1987. An experimental study of subduction and slab migration. J. Geophys. Res. 92, 13,832–13,840.

Lus, W.Y., McDougall, I., Davies, H.L., 2004. Age of the metamorphic sole of the Papuan Ultramafic Belt ophiolite, Papua New Guinea. Tectonophysics 392, 85–101.

Mackwell, S.J., Bai, Q., Kohlstedt, D.L., 1990. Rheology of olivine and the strength of the lithosphere. Geophys. Res. Lett. 17, 9–12.

Mitrovica, J.X., Forte, A.M., 2004. A new inference of mantle viscosity based upon joint inversion of convection and glacial isostatic adjustment data. Earth Planet. Sci. Lett. 225, 177–189. http://dx.doi.org/10.1016/j.epsl.2004.06.005.

Moresi, L., Dufour, F., Mühlhaus, H.-B., 2003. A Lagrangian integration point finite element method for large deformation modeling of viscoelastic geomaterials. J. Comput. Phys. 184, 476–497.

Moresi, L., Quenette, S., Lemiale, V., Mériaux, C., Appelbe, B., Mühlhaus, H.-B., 2007. Computational approaches to studying non-linear dynamics of the crust and mantle. Phys. Earth Planet. Inter. 163, 69–82. http://dx.doi.org/10.1016/j.pepi.2007.06.009.

Müller, R.D., Sdrolias, M., Gaina, C., Roest, R.W., 2008. Age, spreading rates, and spreading asymmetry of the world's ocean crust. Geochem. Geophys. Geosyst. 9, Q04006. http://dx.doi.org/10.1029/2007GC001743.

O'Neill, C., Müller, D., Steinberger, B., 2005. On the uncertainties in hot spot reconstructions and the significance of moving hot spot reference frames. Geochem. Geophys. Geosyst. 6, Q04003. http://dx.doi.org/10.1029/2004GC000784.

Patriat, P., Achache, J., 1984. India–Eurasia collision chronology has implications for crustal shortening and driving mechanism of plates. Nature 311, 615–621.

Ritsema, J., van Heijst, H.J., Deuss, A., Woodhouse, J.H., 2011. S40RTS: a degree-40 shear-velocity model for the mantle from new Rayleigh wave dispersion, teleseismic traveltimes, and normal-mode splitting function measurements. Geophys. J. Int. 184, 1223–1236. http://dx.doi.org/10.1111/j.1365-246X.2010.04884.x.

Royer, J.-Y., Sandwell, D.T., 1989. Evolution of the eastern Indian Ocean since the Late Cretaceous; constraints from Geosat altimetry. J. Geophys. Res. 84, 13755–13782.

Sandiford, M., 2007. The tilting continent: a new constraint on the dynamic topographic field from Australia. Earth Planet. Sci. Lett. 261, 152–163. http://dx.doi.org/10.1016/j.epsl.2007.06.023.

Sandiford, M., Quigley, M., 2009. TOPO-OZ: insights into the various modes of intraplate deformation in the Australian continent. Tectonophysics 474, 405–416. http://dx.doi.org/10.1016/j.tecto.2009.01.028.

Schellart, W.P., 2011. A subduction zone reference frame based on slab geometry and subduction partitioning of plate motion and trench migration. Geophys. Res. Lett. 38, L16317. http://dx.doi.org/10.1029/2011GL048197.

Schellart, W.P., Lister, G.S., Toy, V.G., 2006. A Late Cretaceous and Cenozoic reconstruction of the Southwest Pacific region: tectonics controlled by subduction and slab rollback processes. Earth-Sci. Rev. 76, 191–233.

Schellart, W.P., Moresi, L., 2013. A new driving mechanism for backarc extension and backarc shortening through slab sinking induced toroidal and poloidal mantle flow: results from dynamic subduction models with an overriding plate. J. Geophys. Res., Solid Earth 118, 3221–3248. http://dx.doi.org/10.1002/jgrb.50173.

Schellart, W.P., Spakman, W., 2012. Mantle constraints on the plate tectonic evolution of the Tonga–Kermadec–Hikurangi subduction zone and the South Fiji Basin. Aust. J. Earth Sci. 59, 933–952. http://dx.doi.org/10.1080/08120099.2012.679692.

Schellart, W.P., Stegman, D.R., Farrington, R.J., Freeman, J., Moresi, L., 2010. Cenozoic tectonics of western North America controlled by evolving width of Farallon slab. Science 329, 316–319. http://dx.doi.org/10.1126/science.1190366.

Simmons, N.A., Myers, S.C., Johannesson, G., Matzel, E., 2012. LLNL-G3Dv3: global P wave tomography model for improved regional and teleseismic travel time prediction. J. Geophys. Res. 117, B10302. http://dx.doi.org/10.1029/2012JB009525.

Spakman, W., Bijwaard, H., 2001. Optimization of cell parameterizations for tomographic inverse problems. Pure Appl. Geophys. 158, 1401–1423.

Stegman, D.R., Freeman, J., Schellart, W.P., Moresi, L., May, D., 2006. Influence of trench width on subduction hinge retreat rates in 3-D models of slab rollback. Geochem. Geophys. Geosyst. 7, Q03012. http://dx.doi.org/10.1029/2005GC001056.

Turcotte, D.L., Schubert, G., 2002. Geodynamics. Cambridge University Press, Cambridge. 456 pp.

van der Meer, D.G., Spakman, W., van Hinsbergen, D.J.J., Amaru, M.L., Torsvik, T.H., 2010. Towards absolute plate motions constrained by lower-mantle slab remnants. Nat. Geosci. 3, 36–40. http://dx.doi.org/10.1038/NGEO708.

van Hinsbergen, D.J.J., Steinberger, B., Doubrovine, P.V., Gassmöller, R., 2011. Acceleration and deceleration of India–Asia convergence since the Cretaceous: roles of mantle plumes and continental collision. J. Geophys. Res. 116, B06101. http://dx.doi.org/10.1029/2010JB008051.

van Hunen, J., Allen, M.B., 2011. Continental collision and slab break-off: a comparison of 3-D numerical models with observations. Earth Planet. Sci. Lett. 302, 27–37. http://dx.doi.org/10.1016/j.epsl.2010.11.035.

Veevers, J.J., 2000. Billion-Year Earth History of Australia and Neighbours in Gondwanaland. GEMOC Press, Sydney.

Walker, D.A., McDougall, I., 1982. $^{40}Ar/^{39}Ar$ and K–Ar dating of altered glassy volcanic rocks: the Dabi volcanics, P.N.G. Geochim. Cosmochim. Acta 46, 2181–2190.

Worthing, M.A., Crawford, A.J., 1996. The igneous geochemistry and tectonic setting of metabasites from the Emo metamorphics, Papua New Guinea; a record of the evolution and destruction of a backarc basin. Mineral. Petrol. 58, 79–100.